IOPscience iopscience.iop.org

Home Search Collections Journals About Contact us My IOPscience

Gas gun driven dynamic fracture and fragmentation of Ti-6Al-4V cylinders

This content has been downloaded from IOPscience. Please scroll down to see the full text.

2014 J. Phys.: Conf. Ser. 500 112037

(http://iopscience.iop.org/1742-6596/500/11/112037)

View the table of contents for this issue, or go to the journal homepage for more

Download details:

IP Address: 82.14.222.23
This content was downloaded on 20/05/2014 at 22:21

Please note that terms and conditions apply.

Journal of Physics: Conference Series **500** (2014) 112037 doi:10.1088/1742-6596/500/11/112037

Gas gun driven dynamic fracture and fragmentation of Ti-6Al-4V cylinders

D R Jones[1], D J Chapman[1] and D E Eakins[1]

[1] Institute of Shock Physics, Imperial College London, SW7 2AZ, United Kingdom

E-mail: david.jones06@imperial.ac.uk

Abstract.

The dynamic fracture and fragmentation of a material is a complex late stage phenomenon occurring in many shock loading scenarios. Improving our predictive capability depends upon exercising our current failure models against new loading schemes and data. We present axially-symmetric high strain rate (10^4 s^{-1}) expansion of Ti-6Al-4V cylinders using a single stage light gas gun technique. A steel ogive insert was located inside the target cylinder, into which a polycarbonate rod was launched. Deformation of this rod around the insert drives the cylinder into rapid expansion. This technique we have developed facilitates repeatable loading, independent of the temperature of the sample cylinder, with straightforward adjustment of the radial strain rate. Expansion velocity was measured with multiple channels of photon Doppler velocimetry. High speed imaging was used to track the overall expansion process and record strain to failure and crack growth. Results from a cylinder at a temperature of 150 K are compared with work at room temperature, examining the deformation, failure mechanisms and differences in fragmentation.

1. Introduction

The ability to predict the onset of fracture and the resulting fragmentation behaviour of a body is of huge importance to many fields in industry and engineering. In some applications fracture is undesirable, such as in the aerospace and structural engineering industries where being able to avoid material failure is important. Other areas such as the military need models that capture the fracture and fragmentation accurately to enhance the effectiveness of munitions or mitigation. Where conventional platforms such as the tensile split Hopkinson bar can provide useful data on dynamic fracture, the time taken for the sample to reach an equilibrium state typically limits the sample size so that only a single fracture initiates. For full analysis of a whole body the use of axially symmetric geometries such as rings or cylinders uniformly loaded on the inner surface are commonplace [1–3]. In these cases the whole sample is in a uniform stress and strain-rate state. Hence multiple fractures can initiate depending on the material properties as opposed to effects of the loading technique. The interplay between these fracture sites then controls the fragmentation statistics such as size, mass and velocity.

Several methods exist for expanding rings [4], cylinders [5] and spheres [6]. The work presented here utilises a technique developed by the authors that facilitates expansion of cylinders using a gas gun where the temperature of the sample cylinder can be controlled prior to expansion [7, 8]. This technique is unique in this respect, other drive mechanisms such as explosives [9] and the polymer-polymer gas gun method developed by Winter and Prestidge [10]

Content from this work may be used under the terms of the Creative Commons Attribution 3.0 licence. Any further distribution of this work must maintain attribution to the author(s) and the title of the work, journal citation and DOI.
Published under licence by IOP Publishing Ltd

are not suitable for this research. It is shown that this technique can drive large cylinders (dependant on barrel diameter) at radial strain rates of 10^4 s^{-1}. Sample temperatures down to 150 K have been reached in this work. Future efforts with heating are expected to approach 1000 K. Control of the sample temperature will enable isolation and promotion of different failure modes and study of the effects on the resulting dynamic fracture and fragmentation.

In brief, this method uses a steel tangent-ogive (nosecone) shaped part located inside the rear of the cylinder. A polymer projectile is then launched into the cylinder and the resulting impact causes the projectile to deform around the ogive. The radii of the ogive and projectile leading face can be used to control the deformation. As the polymer flows it drives the cylinder outwards from the inside wall creating a uniform region of axially symmetric expansion. Unlike the Winter and Prestidge method the ogive insert is not required to deform and can be used to house temperature control apparatus. For cooling, low temperature gas or cryogenic liquids are flowed through the ogive, where for heating a resistive heater is placed inside. Both examples conduct heat through the ogive and the cylinder. As the projectile temperature is independent of the cylinder temperature the expansion drive remains constant between experimental conditions.

2. Materials and Experiment

Cylinders were machined from solid rod stock Ti-6Al-4V (% wt.) with the rotational axis aligned with the extrusion direction. Each sample cylinder was 150 mm long, 50 mm inner diameter with a wall thickness of 4 mm. Projectiles of PC1000 polycarbonate, 48 mm outer diameter, 150 mm long with a 50 mm radius concave leading face were launched with a sabot. The ogive was machined from EN24T (AISI 4340) steel with the long radius 37.25 mm. The experiments were performed on the large format 100 mm single stage light gas gun at the Institute of Shock Physics, Imperial College London. The cylinder was mounted in a sleeve which facilitates concentric and tilt adjustments respective to the gun barrel. Alignment was completed using a barrel plug that also enabled accurate measurement of the distance from the diagnostics trigger pin to the point of impact between the projectile and ogive.

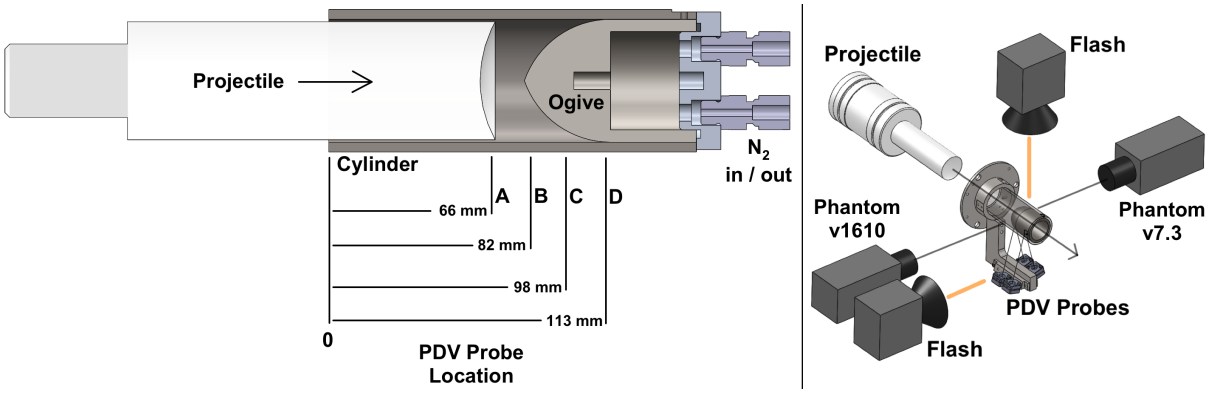


Figure 1. *Left:* Section of projectile and target geometry with the location of PDV probes along cylinder and cooling chamber. *Right:* Location of cameras and lighting.

2.1. Diagnostics

To assist in modelling and simulation efforts it is necessary to record the projectile velocity, cylinder expansion velocity and the onset of failure. The large size of the target tank on the ISP 100 mm gun allows the use of photon Doppler velocimetry (PDV) [11], high speed imaging and soft recovery on the same experiment. Expansion velocity was measured using four channels of frequency-shifted PDV [12] in a line along the cylinder around the region where models

predicted expansion would occur. Focusing probes with a Ø7.2 mm lens and 100 mm focal length in kinematic mounts were staggered on a boom ∼15 mm apart (figure 1). The cylinder surface was polished to a slightly diffuse surface to assist reflection, experiments were performed with 5 mW power delivered to the probes. A single channel of homodyne PDV with a collimating probe was aimed at the sabot to measure impact velocity and provide a reference for the time of impact on the ogive. The target tank has three ports, two of which were used for imaging and one for extra lighting. A Phantom v7.3 was silhouette lit to be used for edge detection and provide the full expansion profile along the same edge observed by the PDV probes. A Phantom v1610 was front lit to measure strain to failure and track crack growth. Lighting was provided by two Bowens Gemini units, one 1500W (side port) and one 1000W (top port). A diagram of the optical setup is shown in figure 1 (right).

2.2. Cooling apparatus

The cylinder was cooled using a pressurised LN_2 system to flow low temperature gaseous N_2 through the hollow in the rear of the ogive. This was fed through a regulator and a remotely operated shut off valve into the target tank through a PEEK flange to aid thermal isolation. Copper tubing was used to transport the gas to the cylinder inside the tank (figures 2 and 3). In future experiments a condensation trap will be used as there was slight icing on the cylinder due to residual moisture in the target tank. Thermocouples were bonded along the cylinder using a low temperature epoxy that remains slightly pliable when set to allow for thermal contraction.

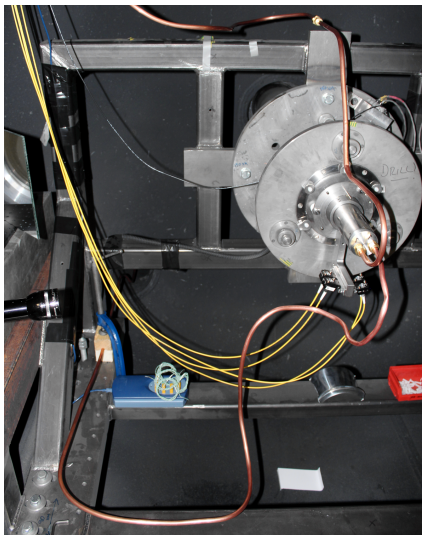


Figure 2. Target tank N_2 feed.

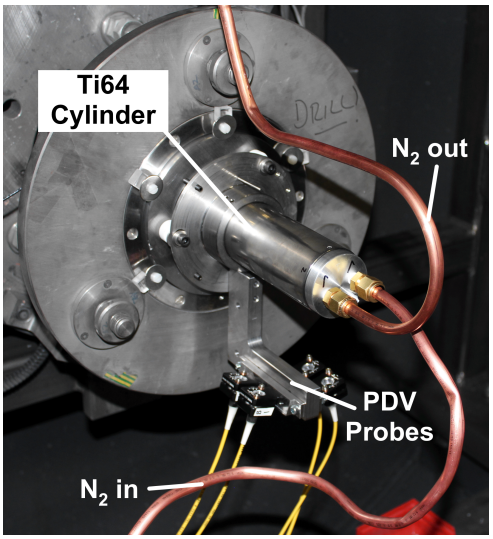


Figure 3. Ti-6Al-4V Cylinder.

The cylinder was isolated from the mounting frame with ceramic spacers. The target tank was evacuated prior to flowing the N_2 into the system. The minimum temperature reached on the cylinder surface was 130 K, with the region of interest (the expansion region) reaching ∼150 K after 30 minutes. The data suggests an equilibrium temperature of 120 K would be possible after more time, however this was beyond the capacity of the nitrogen dewar.

3. Results

An experiment was performed with the expansion region at a temperature of 150±20 K. Projectile velocity was 1001±5 ms^{-1}. This data is compared with an identical experiment with the cylinder at room temperature. Radial velocity and radial strain as measured by the four PDV channels are shown in figure 4.

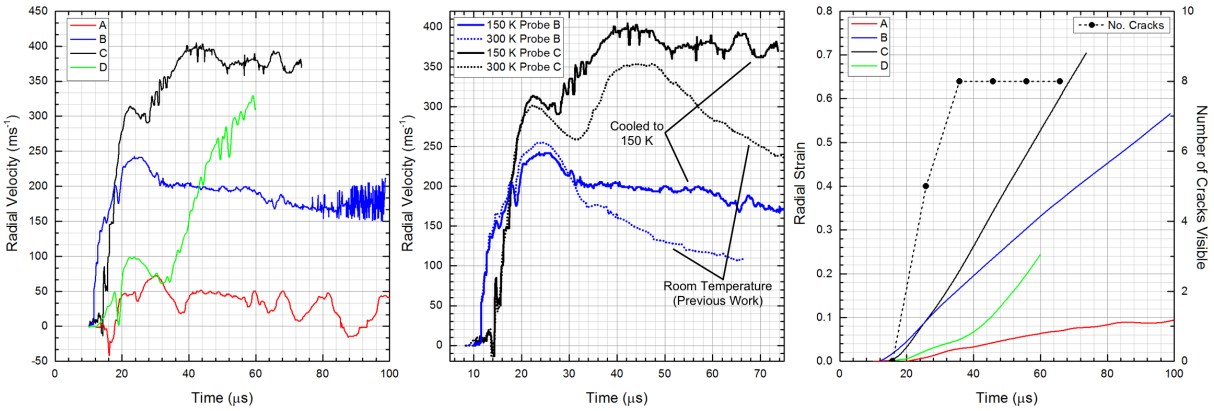


Figure 4. PDV data, **A** - **D** as located in figure 1. *Left*: Radial Velocity. *Centre*: Comparison of probes **B** & **C** for 150 K and 300 K temperature. *Right*: Radial Strain and no. of cracks.

It is clear that expansion initiated between probes **B** and **C**, the locations of which are given in figures 1 and 5. The times given on the plots and images presented here are taken as time after the impact of the projectile on the ogive insert. An instantaneous radial strain rate is defined as

$$\dot{\varepsilon}_r = \dot{r}(t)/r(t) \tag{1}$$

where $r(t)$ is the radius of the outer cylinder wall at a point with time [13]. Peak radial strain rate was measured by probe **C** as 1.02×10^4 s^{-1} at 22.5 μs. The reloading seen in trace **C** at 28 μs is a feature of the geometry, as the polycarbonate translates along the cylinder length the wall is further accelerated. The centre plot compares radial velocity data from this experiment at 150 K (solid lines) with previous work at 300 K (dotted). It is clear in the cooled case that there is far less deceleration of the cylinder wall from 30 μs for **B** and 45 μs for **C**. This suggests that the cooled cylinder is failing earlier and hence loses strength, providing less resistance to the expansion, confirmed in the high speed imaging. The radial strain plot (right) demonstrates the symmetry of the expansion process. Probes **A** and **D** are approximately equally spaced around the expansion peak, as are **B** and **C**. The radial strain histories are in very close agreement until the time at which there is considerable failure in the cylinder, between 35 and 45 μs. Further evidence of a highly symmetric bell-shaped expansion profile is given in the high speed imaging data in figure 5. Once sufficient deformation and fracture has occurred the longitudinal cracks merge and the cylinder effectively bifurcates. The material downstream of the projectile path is further loaded by the expanding polycarbonate, as seen by the large radial velocity reached by probe **D** later in time.

Figure 5 shows the images recorded by the front-lit Phantom v1610 for the 150 K cylinder. From analysis of the high speed imaging from the two experiments it is clear that fracture initiated much earlier in the cooled cylinder, causing a loss of strength and hence less deceleration of the expansion velocity. This is a result of the reduced ductility of the Ti-6Al-4V in the cooled experiment. Up to this point the velocity histories are very similar for the two temperatures, showing that this expansion technique is capable of repeatable uniform loading independent of the sample temperature. From the plot showing the number of cracks with radial strain (figure 4, right) it is shown that the majority of fracture sites appeared before 10% radial strain was reached. However, these cracks do not fully penetrate the wall until around 15-20% strain. This is in agreement with the earlier fracture predicted from comparison of the PDV data between this 150 K work and the previous 300 K where failure initiated at around 22% strain.

Figure 6 shows the recovered fragments and a detail of the internal damage seen in several

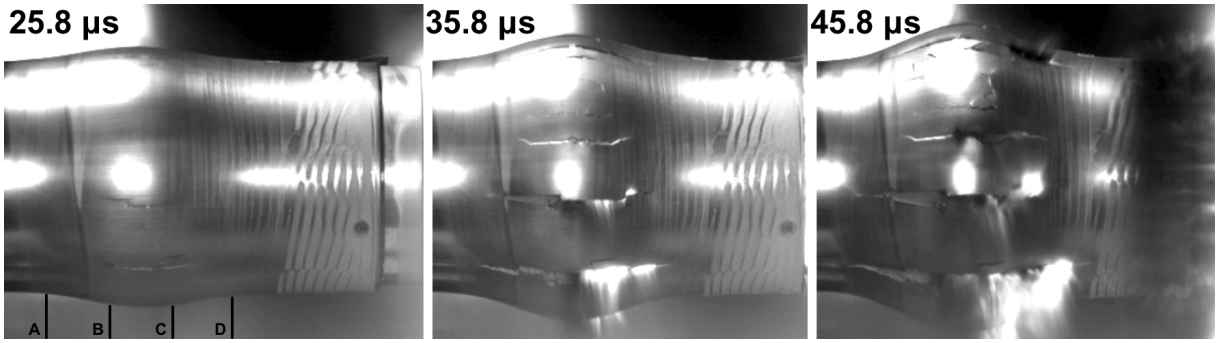


Figure 5. Images from the Phantom v1610, 150 K cylinder. Projectile enters from the left. Location of PDV probes shown in first frame. Icing visible on the end of the cylinder.

fragments. The dominant failure mode observed was through longitudinal cracking at 45° to the radius, producing long thin fragments around the region of expansion. The failure mechanism was identified as ductile shear fracture from this 45° orientation and the elongated parabolic dimples in the SEM imaging (inset 2). However, unseen in the work at room temperature, there was also internal damage generated in the cylinder wall with the material separating in a similar way to a spall fracture (inset 1). This was confirmed with SEM showing circular dimples consistent with tensile failure.

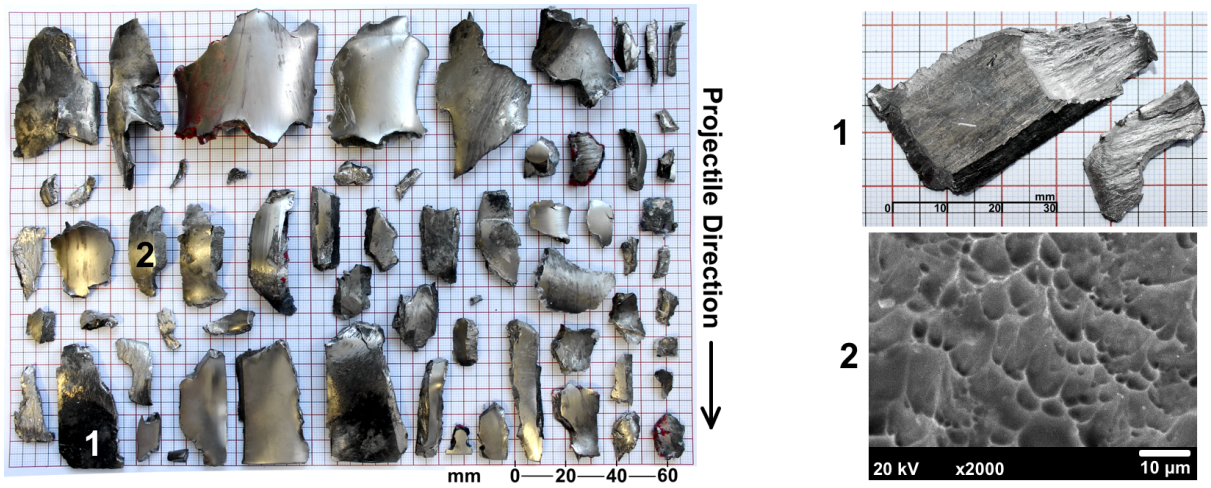


Figure 6. *Left*: Reconstruction of recovered fragments with projectile direction, outer cylinder wall side shown. *Right, 1*: Detail of fragment 1 showing spall damage. *2*: SEM of fracture surface of fragment 2.

4. Conclusions / Future Work

The work presented here represents novel data generated using a technique for study of the temperature sensitive dynamic ductility, fracture and fragmentation behaviour of a material. This data is not currently attainable using other expansion drives such as high explosives or the classic polymer-polymer based gas gun method. A Ti-6Al-4V cylinder, inner diameter 50 mm and 4 mm wall thickness has been uniformly expanded to failure at a radial strain rate of 10^4 s^{-1}. Expansion velocity was recorded at multiple points with PDV in conjunction with

high speed imaging to provide a complete record of the deformation behaviour and onset of failure. Fracture was found to initiate earlier in this cooled work than previous work with room temperature samples. In addition to the typical shear related failure observed there was also evidence of an internal tensile damage mechanism occurring in the cylinder wall. The possibility of this being related to spall needs further investigation. This data will be of great use in assisting hydrocode modelling and simulation efforts.

Acknowledgements
The authors and the Institute of Shock Physics gratefully acknowledge continued funding and support for the project from the Atomic Weapons Establishment (AWE) and Imperial College London (ICL). Samples were prepared by the Physics Mechanical Instrumentation Workshop (ICL). The Phantom v1610 used was kindly provided by Vision Research.

References

[1] Mott N 1947 *Proc. R. Soc.* A **189** 300-308
[2] Hoggatt C R and Recht R 1968 *J. Appl. Phys.* **39** 1856-1862
[3] Grady D E and Benson D A 1983 *Exp. Mech.* **23** 393-400
[4] Goto D M, Becker R, Orzechowski T J, Springer H K, Sunwoo A J and Syn C K 2008 *Int. J. Imp. Eng.* **35** 1547-1556
[5] Vogler T 2003 *Int. J. Imp. Eng.* **29** 735-746
[6] Balagansky I A, Karanik Y A, Agureikin V A and Vinogradov A V 2001 *Theor. Appl. Fract. Mech.* **36** 165-173
[7] Jones D R, Eakins D E, Hazell P J, Chapman D J and Appleby-Thomas G J 2012 *AIP Conf. Proc.* **1426** 1141-1144
[8] Jones D R, Chapman D J and Eakins D E 2013 *J. Appl. Phys.* **114** 173508
[9] Famiglietti M 1952 *Ballistic Research Laboratories Report* **BRL-MR-597**
[10] Winter R and Prestidge H 1978 *J. Mat. Sci.* **13** 1835-1837
[11] Strand O T, Goosman D R, Martinez C, Whitworth T L and Kuhlow W W 2006 *Rev. Sci. Inst.* **77** 083108
[12] Mercier P, Bénier J, Frugier P A, Sollier A, Le Gloahec M R, Lescoute E, Cuq-Lelandais J P, Boustie M, De Resseguier T and Claverie A 2009 *AIP Conf. Proc.* **1195** 581
[13] Hoggatt C R and Recht R F 1969 *Exp. Mech.* **9** 441-448